

Feasibility of determining the quantitative OH content of garnets with Raman spectroscopy

ELIZABETH H. ARREDONDO* AND GEORGE R. ROSSMAN

Division of Geological and Planetary Sciences California Institute of Technology, MS 170-25, Pasadena, California 91125, U.S.A.

ABSTRACT

Two suites of garnets were examined by infrared absorption spectroscopy and depolarized Raman spectroscopy to determine if the Raman signal could be used as a quantitative measurement of OH content. To avoid the problems of determining the absolute Raman signal intensity, the integrated intensity of the OH bands was ratioed to the integrated intensity of silicate Si-O stretching bands and used as a proxy for the OH intensity. These were compared to the OH contents, expressed as wt% H₂O, independently determined from infrared absorption. A somewhat useful trend developed between OH contents determined by Raman and IR for some grossular garnets with H₂O contents less than 0.5%. Many colorless to near-colorless grossular garnets do not provide a useful Raman signal due to fluorescence, although other samples with H₂O contents between 0.5 and 1.3 wt% and are strongly colored, fall far below the trend of the samples with lower H₂O-contents. Spessartine-almandine garnets from the Rutherford no. 2 pegmatite all respond to the Raman experiment, but produce a confusing trend when compared to H₂O. Coincidentally, a relatively smooth but decreasing trend was observed when the spessartine Raman OH intensity ratio was compared to the iron content. These observations suggest that Raman measurements by this method are not suitable, in general, for the determination of OH in garnets.

INTRODUCTION

Hydroxide ions are a minor component of many silicate minerals that are usually formulated as anhydrous. In garnets, the concentration of OH can range from trace levels to that of a major component. Hydroxyl in garnet has been extensively studied with infrared transmission spectroscopy, and analytical calibrations have been established through integrated absorbance and peak heights for the spessartine-almandine series (Rossman et al. 1988), for grossular (Rossman and Aines 1991), and for pyrope (Bell et al. 1995). Although infrared methods are comparatively easy to conduct, they do require that the sample be prepared as a doubly polished slab of thickness appropriate for the amount of OH in the sample. Because Raman spectroscopy is a relatively fast and easy way to collect data with minimal sample preparation, we wanted to evaluate the utility of this method to acquire quantitative OH concentrations for some members of the garnet family. Available for this study were the suite of grossular samples used by Rossman and Aines (1991) in their study of OH in grossular, and the suite of spessartine-almandine garnets from the Rutherford no. 2 pegmatite used by Arredondo et al. (2001). Analyses by Raman spectra have proven useful for determining water contents of melt inclusions in granite with contents ranging from 0–20 wt% (Thomas 2000). The goal of this project was to determine if Raman spectra could provide the same quantitative measure of OH contents that can now be obtained by infrared transmission spectra.

EXPERIMENTAL METHODS

Sample description

Forty-one grossular and ten spessartine-almandine garnets with OH concentrations previously determined by infrared spectroscopy were analyzed for this study. The grossular garnets range from colorless to green to brown-orange. Their OH concentrations (expressed as wt% H₂O), previously determined by Rossman and Aines (1991), range from 0.023 to over 13 wt% H₂O, with certain samples having approximately 9 to 12 OH per formula unit. The spessartine-almandine garnets range from deep red (Sp₄₅) to pale orange (Sp₉₁) in color. Their OH concentrations, determined by Arredondo et al. (2001), range from 0.02 to 0.16 wt% H₂O. Full descriptions of the samples in Table 1, including compositions, are presented in Rossman and Aines (1991) and Arredondo et al. (2001).

Infrared OH analysis

When needed, re-analyses of samples used in prior studies were conducted on a Nicolet Magna 860 FTIR operating at 4 cm⁻¹ resolution. Each sample was doubly polished and the clearest portion was mounted over a steel pinhole aperture ranging from 100 to 400 micrometers in diameter. Hydroxyl contents were determined from the integrated area of the OH stretching bands as detailed in Rossman and Aines (1991), and Arredondo et al. (2001).

* E-mail: miura@gps.caltech.edu

TABLE 1. Sample descriptions and analytical results

Sample no.	Locality	OH/Si	Fluorescence Yes/No	wt% H ₂ O
Grossular*				
42	Ramona, California, U.S.A.	0.0397	N	0.10
52	Vesper Peak, Washington, U.S.A.	0.0220	N	0.14
53	Asbestos, Quebec, Canada		Y	0.21–0.38
771	Meralini Hills, Tanzania		Y	0.18
936	Bric Camula, Cogoletto, Liguria, Italy	0.1578	N	1.26
937	Passo del Faiallo, Genova Province, Liguria, Italy	0.1734	N	1.01
941	Buffelsfontein, Rustenberg, South Africa	2.7906	N	N/A
946	Auerbach, Germany	0.0533	N	0.26
1051	Eden Hills, Vermont, U.S.A.		Y	0.02–0.04
1037	Dos Cabezas, Imperial County, California, U.S.A.		Y	0.06
1113	North Hill, Riverside, County, California, U.S.A.	0.0404	N	0.09
1124	Chihuahua, Mexico		Y	0.11
1122	Crestmore, California, U.S.A.	0.0285	N	0.13
1125	Lake Jaco, Mexico		Y	0.03
1129	Belvidere Mountain, Vermont, U.S.A.	0.1575	N	0.53
1131	Lake Jaco, Mexico		Y	0.01
1198	Transvaal, South Africa	1.3772	Y	3.59
1326	Ala Valley, Piedmont, Italy	0.0874	N	0.37
1327	Sciarborosca, Liguria, Italy	0.1662	N	0.47
1329	Commercial Quarry, Crestmore, California, U.S.A.	0.1722	N	N/A
1357	Bric Canizzi, Liguria, Italy	0.1974	N	0.43
1359	Iron gabbro metaroddingite, Gruppo di Voltri, Italy		Y	0.28
1360	Basaltic metaroddingite, Voltri Massif, Italy	0.1897	N	0.85
1411	Skarn, Munam, North Korea	0.0173	N	0.08
1412	Mul-Kum mine, South Korea		Y	0.10
1419	Minot Legde, Minot, Maine, U.S.A.	0.0209	N	0.16
1420	Rauris, Salzburg, Austria	0.0614	N	0.26
1422	Wakefield, Ontario, Canada		Y	0.02
1413	Vilyi River, Siberia, Russia		Y	0.0003
1423	Mountain Beauty mine, Oak Grove, California, U.S.A.		Y	0.06
1424	Santa Rosa Mountains, California, U.S.A.	0.0499	N	0.17
1429	Essex County, New York, U.S.A.		Y	0.05
1444	Pietramassa, Viterbo, Italy		Y	N/A
Spessartine-almandine †				
R2G1	Amelia, Virginia, U.S.A.	0.0128	N	0.023
R2G2	Amelia, Virginia, U.S.A.	0.0088	N	0.022
R2G3	Amelia, Virginia, U.S.A.	0.0453	N	0.083
R2G4	Amelia, Virginia, U.S.A.	0.0237	N	0.127
R2G5	Amelia, Virginia, U.S.A.	0.0450	N	0.13
R2G6	Amelia, Virginia, U.S.A.	0.0475	N	0.134
R2G7	Amelia, Virginia, U.S.A.	0.0547	N	0.130
R2G8	Amelia, Virginia, U.S.A.	0.0493	N	0.158
R2G9	Amelia, Virginia, U.S.A.	0.0639	N	0.147
R2G10	Amelia, Virginia, U.S.A.	0.0662	N	0.121

* Grossular descriptions and wt% H₂O taken from Rossman and Aines (1991).

† Spessartine-almandine descriptions and wt% H₂O taken from Arredondo et al. (2001).

Raman spectroscopy

Each sample was analyzed on a Renishaw Micro Raman spectrometer operating with a 514.5 nm argon ion laser, with spectral resolution of 1 cm⁻¹. Because Raman spectra of solids in general, and garnets in particular (Kolesov and Geiger 1997) are subject to polarization effects, a double wedged quartz depolarizer was placed in the instrument to minimize the effects of polarization in the Raman experiment. All samples were doubly polished slabs used in previous IR spectroscopy studies. No additional sample preparation was needed for the Raman measurements. The diameter of the spot used for collection varied from 4 to 40 micrometers depending on the quality of the sample's surface. Scan times and number of accumulations were chosen to provide adequate signal to noise ratios in the OH region. Typical Raman spectra of grossular and spessartine-almandine are presented in Figure 1.

The analytical approach was to determine the ratio of the integrated absorbance of the depolarized Raman bands in the ~3600 cm⁻¹ OH stretching region to the integrated absorbance of the bands in the 800–900 cm⁻¹ Si-O stretching region (here-

after referred to as the OH/Si ratio). Absolute intensities were not used because Raman intensities generally depended on the quality of the sample's surface polish and the alignment of the instrument. These ratios were then compared to the quantitative wt% H₂O measurements previously obtained from the infrared spectral measurements. To test the quality of the depolarization, we conducted a series of tests on six samples of spessartine and grossular that span the range of water contents. These tests involved re-acquisition of the Raman spectrum after the sample stage was rotated through a series of angles. These results showed that the low water content samples of both grossular and spessartine have a 3–15% change in the OH/Si ratio. These variations are not significant in the context of this paper in view of the much larger effects described in the results section. An oriented sample of spessartine showing the (100) face was also analyzed through the series of rotation angles to try and maximize the residual polarization effects within the instrument. We found only a 12.5% difference in the OH/Si ratio. Only one sample from the Rossman and Aines (1991) paper was ex-

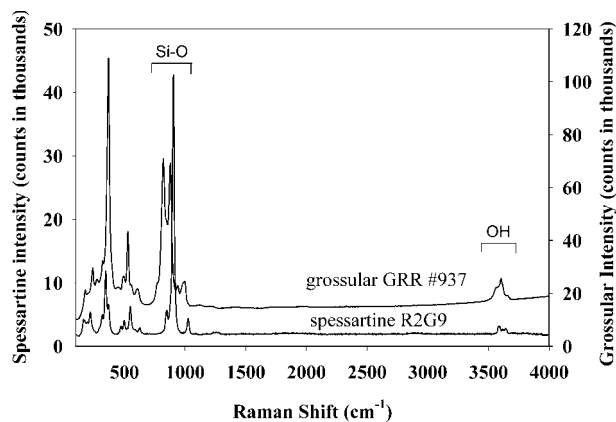


FIGURE 1. Typical Raman spectra of a grossular (GRR #937) and a spessartine-almantine garnet (R2G9), showing the OH and Si-O regions used for analyses. (Grossular spectrum has been offset for clarity.)

cluded from this study. The highest water content sample (GRR no. 1198) showed a 50% change in OH/Si ratio. We also checked the homogeneity of the OH absorbance peak in the infrared and found it varied significantly.

RESULTS

All of the spessartine-almantine garnets provided useful Raman signals in the OH stretching region (Fig. 1). Fourteen of the grossular samples could not be used due to laser induced sample fluorescence. Neither suite of garnets provided a consistent correlation of OH/Si ratio with H₂O concentration. Furthermore, the two suites did not give the same trend.

Figures 2a and 2b show the OH/Si ratio of the grossular samples vs. wt% H₂O. There is a general trend of increasing OH/Si ratio with increasing H₂O content up to about 0.5 wt%. Above 0.5 wt% the trend changes to a nearly constant plateau for the garnets between 0.8 and 1.3 wt%. Figure 3 shows the integrated absorbance ratio of OH vs. wt% H₂O in the spessartine-almantine garnets. This trend shows greater scatter in the higher H₂O concentration than the grossular trend.

DISCUSSION

To examine what factors contributed to the scatter in these results, a variety of correlations were examined. The first factor considered was the iron content in both grossular and spessartine-almantine garnets. Optical spectra were taken of one high iron spessartine-almantine (R2G2 = 1.682 mol% Fe) and one low iron (R2G10 = 0.163 mol% Fe) sample, to see where the laser line and the Raman emission are absorbed (Fig. 4). From this we can compare the differences in absorption of the two samples. At the laser line (514.5 nm) we see a much higher absorption compared to the OH Raman emission at 630 and 633 nm, as well as a difference in absorption in the high and low iron samples. Figure 4 shows that even though there is a significant difference between the high and low iron samples, the amount of attenuated light is negligible over the volume in which the signal is generated. Less than one one-hundredth of one percent of the Raman emission is being lost over the few

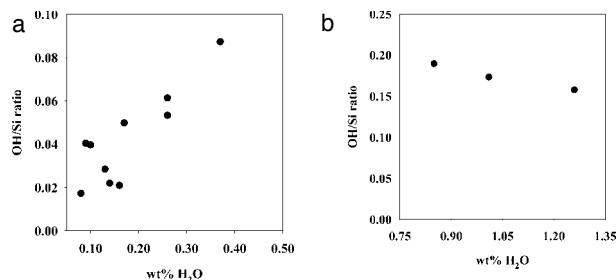


FIGURE 2. (a) OH/Si ratio vs. wt% H₂O for low water content grossular garnets. (b) OH/Si ratio vs. wt% H₂O for high water content grossular garnets.

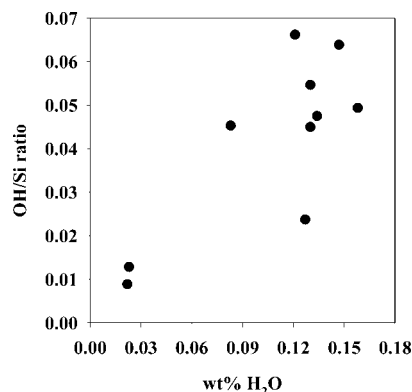


FIGURE 3. OH/Si ratio vs. wt% H₂O for the spessartine-almantine garnets.

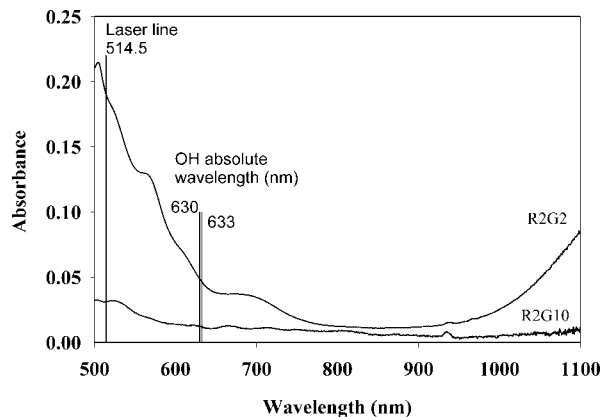


FIGURE 4. Optical absorption spectra of a high- and low-iron spessartine-almantine garnet, showing where the laser line and OH Raman emissions occur in the spectra. Spectra were normalized to 0.200 mm thickness.

micrometer thickness penetration into the sample.

If the wavelength of the incident laser coincided with an optical absorption band of either Mn or Fe in the garnets the OH signal in iron-containing garnets could potentially be intensified due to the resonance Raman effect. In the spessartine-almantine series, the iron content is correlated to the OH/Si ratio but with a decreasing trend (Fig. 5). The direction of the

trend makes the resonance Raman effect unlikely, but raises the possibility that absorption of the Raman OH signal at 630–633 nm by the sample might be a factor. However, the Si-O emission in the 540 nm region is more strongly absorbed by the iron, so the observed trend of the OH/Si ratio is in the wrong direction for this to be the cause. Furthermore, the levels of absorbance from Figure 4 indicate that the absolute amount of light being absorbed by the samples is negligible over the short path traversed. For grossular, the iron content is not correlated to the OH/Si ratio (Fig. 6). There are two reasons why the difference between the two garnet species is so pronounced. First, the spessartine-almandine garnets have much more iron compared to the grossulars in this study, and in the grossulars much of the iron is Fe^{3+} whereas it is nearly entirely Fe^{2+} in the spessartine-almandine garnets.

Color was also considered. The grossular samples have a much greater range of colors (colorless, green, red-orange),

whereas the spessartine-almandine samples were red to light orange. Of the pale to colorless grossular samples only three of the twelve that were analyzed gave a spectrum adequate to use for these correlations. The others generated so much fluorescence with the 514.5 nm excitation wavelength that they could not be used. The OH/Si ratios derived from the spectra of colored and non-colored garnets were examined separately (Fig. 7). Although there is no overall correlation, it is apparent that the garnets with greater than 0.8 wt% H_2O that deviated from the general trend established by the lower H_2O -content samples, were all colored.

To test if different types of OH responded differently, samples that have spectra in the OH region with a significant contribution from lower wavenumber bands (3548–3572 cm^{-1}) were also considered separately. This did not provide a better correlation (Fig. 8). One potential uncertainty arises from the fact that Rossman and Aines (1991) independently calibrated

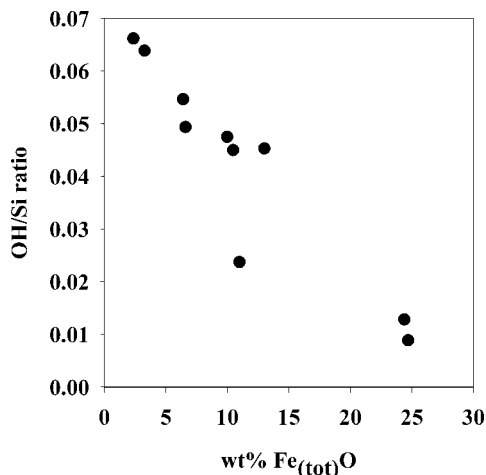


FIGURE 5. OH/Si ratio vs. wt% $\text{Fe}_{(\text{tot})}\text{O}$ for the spessartine-almandine garnets.

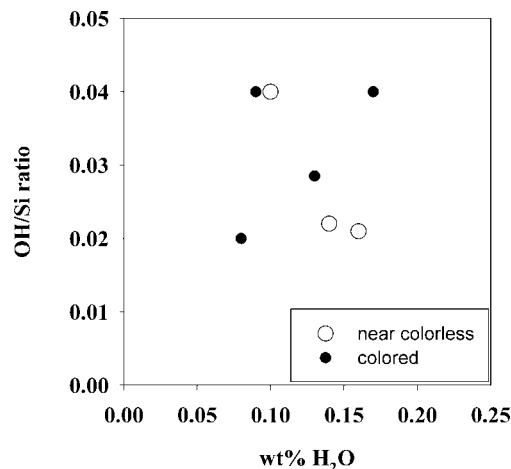


FIGURE 7. OH/Si ratio vs. wt% H_2O for colored and near colorless grossular garnets.

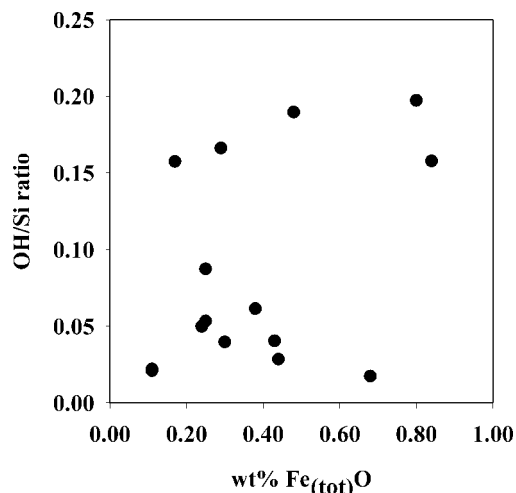


FIGURE 6. OH/Si ratio vs. wt% $\text{Fe}_{(\text{tot})}\text{O}$ for the grossular garnets.

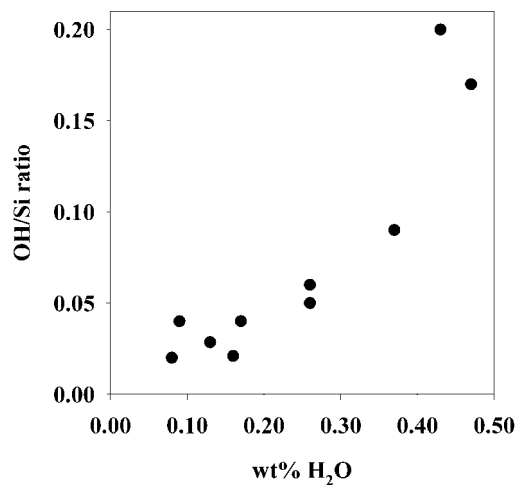


FIGURE 8. OH/Si ratio vs. wt% H_2O for grossular garnets with low wavenumber OH bands (3548–3572 cm^{-1}).

only a small subset of the grossular garnets in their study. Garnets have complex OH spectra in both IR transmission and Raman spectroscopy. In spite of our test with the lower wavenumber OH bands described above, it could still be the case that different OH peaks contribute unequally whereas it was assumed that they all have equal contributions. Homogeneity can also be a problem. Many samples have inhomogeneous OH contents. This is a greater problem with the infrared measurements because of the greater volume of the sample that is interrogated. The Raman measurement can be confined to a smaller volume, but if the OH content in the volume of the Raman experiment were different than the volume used for the IR measurement, the results would not correlate.

Although a subset of the lower water content grossulars give a semi-consistent trend of increasing OH/Si ratio with H₂O content, it is not possible to know a priori if any individual garnet is a member of this subset. The spessartine trends are of little analytical use. These observations suggest that, at this time, Raman measurements by this method are not generally suitable for the quantitative determination of trace amounts of OH in garnets.

ACKNOWLEDGMENTS

This study was made possible through the support of the National Science Foundation, grant EAR-9804871, and the White Rose Foundation. We thank B. Kolesov and an anonymous referee for helpful comments that improved the manuscript.

REFERENCES CITED

- Arredondo, E.H., Rossman, G.R., and Lumpkin, G.R. (2001) Hydrogen in spessartine-almandine garnets as a tracer of granitic pegmatite evolution. *American Mineralogist*, 86, 485–490.
- Bell, D.R., Ihinger, P.D., and Rossman, G.R. (1995) Quantitative analysis of hydroxyl in garnet and pyroxene. *American Mineralogist*, 80, 465–474.
- Kolesov, B.A. and Geiger, C.A. (1997) Raman scattering in silicate garnets: an investigation of their resonance intensities. *Journal of Raman Spectroscopy*, 28, 659–662.
- Rossman, G.R. and Aines, R.D. (1991) The hydrous components in garnets: grossular-hydrogrossular. *American Mineralogist*, 76, 1153–1164.
- Rossman, G.R., Rauch, F., Livi, R., Tombrello, T.A., Shi, C.R., and Zhou, Z.Y. (1988) Nuclear analysis of hydrogen in almandine, pyrope, and spessartite garnets. *Neues Jahrbuch für Mineralogie Monatshefte*, 172–178.
- Thomas, R. (2000) Determination of water contents of granite melt inclusions by confocal laser Raman microprobe spectroscopy. *American Mineralogist*, 85, 876–872.

MANUSCRIPT RECEIVED FEBRUARY 19, 2001

MANUSCRIPT ACCEPTED NOVEMBER 7, 2001

MANUSCRIPT HANDLED BY M. DARBY DYAR